Comparative study of permanent magnet synchronous machine vs salient pole synchronous machine in high temperature application

Romain Cousseau, Raphaël Romary, François Balavoine, Miftah Irhoumah, Remus Pusca

Comparative study of permanent magnet synchronous machine vs salient pole synchronous machine in high temperature application

Romain COUSSEAU, Raphaël ROMARY, François BALAVOINE, Miftah IRHOUMAH, Remus PUSCA
Univ. Artois, UR 4025, Laboratoire Systèmes Electrotechnique et Environnement (LSEE)
F-62400 Béthune, France
romain.cousseau@univ-artois.fr

***Abstract*—This paper presents the sizing and the comparison of two synchronous machines. The purpose is to design a high temperature dedicated machine with the same performance and volume as a permanent magnet machine. To compare the machines, torque has been chosen as a reference indicator and not the efficiency which will be not so good for the high temperature machine. A salient pole wound rotor is chosen with anodized aluminum tape as windings. Works presented should be considered as preliminary studies leading to the conception of a prototype.**

Keywords— Motor sizing, high temperature, permanent magnet, anodized aluminum tape, thermal study.

1 INTRODUCTION

In a large variety of fields, electrical machines are more and more preferred to traditional actuators (pneumatics or hydraulics) [1]. Indeed, thanks to their compactness and efficiency, machines like PMSM (Permanent Magnet Synchronous Machine) are very attractive [2][3]. However, because of the use of permanent magnets, this kind of machine is not very suitable in high temperature operating conditions [4].

The field of high temperature machine design has been specially investigated during the last decade [5]. Two different applications of high temperature winding are identified, the first one is related to operation in a harsh environment where the external temperature can be very high, like aircraft application with the concept of More Electric Aircraft (MEA) [6] where electrical machines operated in an environment with high ambient temperature (more than 200°C [1]). The second one concerns machine designed with high power density where line current and surface current density are very high [7]. In addition to the issue of magnet demagnetization, the other weak point of high temperature machines is related to wire insulation. Organic insulation using Polyamide Imide (PAI) and Polyester Imide (PEI) material does not allow to exceed 200°C at the hottest point of the machine (the conducting copper). To go beyond this limit, inorganic insulation can be an alternative solution [8][9][10], like ceramic copper wire, nickel-plated copper wire, or anodized aluminum tape. However, the mechanical characteristic of inorganic insulation is different than this of PEI-PAI; what requires specific know-how in winding and machine building, which can bring real manufacturing difficulties. Anodized aluminum tape has a real advantage in high temperature machine design [11]. Firstly, the aluminum is flexible and enables a low bending radius which make it easier to wind the coil. Therefore, an Anodized aluminum coil fits well with a concentrated winding machine. The inter-turn voltage is well controlled, and the anodized layer insure a good inter turn insulation to more than 350°C. The anodized aluminum strip has also the advantage to be available in the marketplace at different wanted dimensions (width, thickness).

The aim of this paper is to present the sizing of two machine topologies of 40 kW for 4500 rpm with similar sizes and performances. The purpose is to lead to the design of a laboratory prototype that could fit with aircraft or car industries requirements. The first machine is made with a permanent magnet rotor whereas the other one is made with a salient pole wound rotor to operate at high temperature. The second machine uses anodized aluminum tape [12][13] as windings. The stator windings use the same conductor to hold the high temperature.

The paper is organized as follows: Section 2 presents the sizing of a three-phase 12/10 (12 slots, 10 poles) synchronous machine with a concentrated winding. Section 3 gives comparisons between the two machines through finite element simulations. Section 4 presents a complete thermal study for both machines. Section 5 brings an explanation of the wound rotor construction. Section 6 gives conclusions and highlights works that will be made for the future machine that is currently being built.

2 SIZING AND DESIGN OF THE MACHINES

2.1 Main dimensions

First, it is necessary to find the main dimensions of the machine as a preliminary sizing process. The purpose is not to optimize the compacity of the machine but to get an easily achievable electrical motor. To achieve that, the sizing formula in (1) is used. This is a simplified version of the sizing equation given in [14].

$$D_a{}^2 L_a = \frac{2C}{A\hat{B}\frac{K_1^s \pi}{\sqrt{2}}} \tag{1}$$

With D_a: the inner diameter of the stator, L_a: the active length, C: the rated torque, A: the current linear density, B: the peak airgap flux density and $K_1{}^s$: the winding factor.

The winding factor depends on the chosen topology such as the number of phases, slots and poles as explained in [15]. Considering (1), parameters are chosen as well as the active length to obtain a coherent stator diameter. The purpose is to

obtain a mean torque of 100 Nm in a 0-4500 rpm speed range for two machines: the first one is a reference machine with a permanent magnet rotor that will be considered in the design process. The second machine has the same dimension as the reference one but with a wound rotor designed to provide the same magnetic effect than the permanent magnet rotor. In order to reach the same magnetic performance as the initial machine, the wound rotor machine uses anodized aluminum tape able to operate at high temperature (more than 350°C). To simplify, both machines have the same stator with concentrated winding, also made with anodized aluminum tape. Parameters are summed up in Table I, where the Torque C comes from desired specifications described before, the line current density A is a usual design value of permanent magnet machine to achieve acceptable heating [14] because the reference permanent magnet machine is a low temperature one. The peak airgap flux density B has been chosen as the more probably attained regarding magnet characteristic associated with the flux concentrated effect of the rotor magnet configuration. This value will be checked with a finite element simulation. The airgap width has been set to 1 mm which is a reasonable value for manufacturers.

TABLE I. DESIGN PARAMETERS

Torque C	100 Nm
Line current density A	27000 A/m
Peak airgap flux density B	1.5 T
Winding factor K_1^s	0.933
Active length L_a	150 mm

In previous studies about other types of machines, an active length L_a of 150 mm was defined. To keep approximatively the same volume regarding the existing testbench, the choice has been made to keep this characteristic value. This leads to an inner stator diameter of 126 mm.

Magnets have been taken the thickest of possible to be less sensitive to the temperature and to bring the highest flux density in the airgap, considering an interior magnet structure with flux concentration effect. The permanent magnet machine is not supposed to heat over some range; however, it is safer to use SmCo magnets that can handle higher temperature than NeFB magnets. Teeth wide has been determined to be minimum without being saturated.

To determine the external diameter, it is considered that half of the magnetic flux of a rotor pole flows through this part of the machine. Considering the principle of flux conservation, the iron thickness can be calculated. Finally, the external diameter is 206 mm.

2.2 *Winding determination*

The method presented in [15] is used to determine the optimum winding sequence of the concentrated winding machine. The chosen structure of the machine is three-phase 12/10 (12 stator slots, 10 poles) with double layer concentrated winding. At first, the SPP (number of slots per poles and per phase) needs to be determined (2).

$$SPP = 12/(3*10) = 2/5 \quad (2)$$

The purpose is to compare a sequence of "zeros" and "ones" to a reference sequence. According to the method, our comparative sequence will have 2 "ones" and 3 (5-2) "zeros" and will be "01010". The sequence is shown in Fig. 1 and the corresponding winding factor is 0.933.

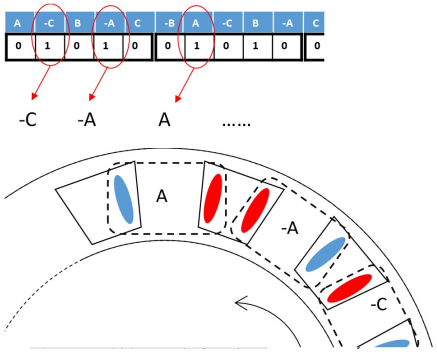

Fig. 1. Determination of the optimal winding sequence

2.3 *Results of the sizing*

Once sizing and winding have been determined, it is possible to draw both machines. Fig. 2 and 3 show the two machine configurations having similar dimensions. For the wound rotor machine, saliencies have been designed to let enough space to place rotor windings. Based on these geometries, finite element simulations with Altair Flux 2D software will be performed in the next section.

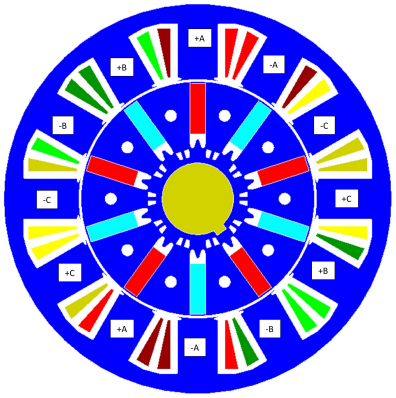

Fig. 2. Permanent magnet configuration

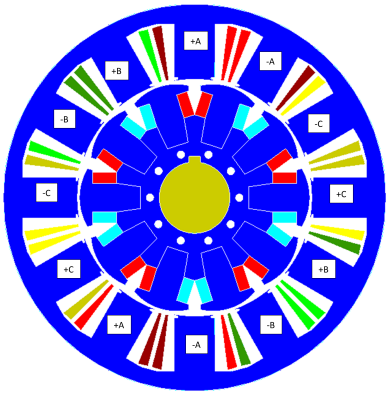

Fig. 3. Salient pole wound rotor configuration

3 COMPARISON OF THE TWO MACHINES WITH FINITE ELEMENT SIMULATION

3.1 Performance comparison using torque and airgap flux density

Performances of the two machines are compared through finite element simulations for the expected rated point (4500 rpm – 100 Nm). These simulations have been made at a constant temperature not considering changes in material characteristics. Thus, electrical resistances are calculated at 20°C.

In a first step, the rotor direct current of the salient pole machine has been determined to achieve roughly the same airgap flux density as the permanent magnet rotor, as shown in Fig. 4. Stator number of turns and stator current are similar for both machines and they are limited by the induced voltage that cannot exceed the DC bus voltage at maximum speed. The machine is powered with sine current and with flux-oriented control. Winding characteristics are summarized below.

- Stator windings: 10 coils per tooth (anodized aluminum tape of 0.4*24 mm)
- Stator current I_s: 80 A peak (56.6 A RMS - 6A/mm² current density)
- Rotor windings: 40 coils per pole (anodized aluminum tape of 0.15*12 mm)
- Rotor current I_r: 30 A direct current (16 A/mm² current density)

Fig. 5 presents the spectrum of the normal flux density in the airgap. As expected, the 5th harmonic is the principal because of the 5 pairs of poles. It is slightly higher for the permanent magnet machine but not significatively. However, some other harmonics like the 15th are higher.

Fig. 6 gives the torque of both machines at rated stator and rotor currents. It can be observed that the target torque was 100 Nm but, in both cases, simulated torques are weaker. This can be accounted for by assumptions used in the sizing formula. For example, the airgap flux density taken at 1.5 T in (1) has roughly this value in the simulation for the peak value in Fig. 4, but the fifth harmonic in Fig. 5 falls to 0.85 T.

Because of the magnet configuration, the PMSM is a flux concentrated machine, that leads to a slightly higher induction in stator teeth (around 1.3 T vs 1.2 T for the wound rotor machine). This can justify that the mean torques are not the same for both machines. Additionally, an interesting point is that the 12th harmonic (which corresponds to the number of slots) is the main one for the PMSM torque ripple whereas it is the 6th for the other rotor.

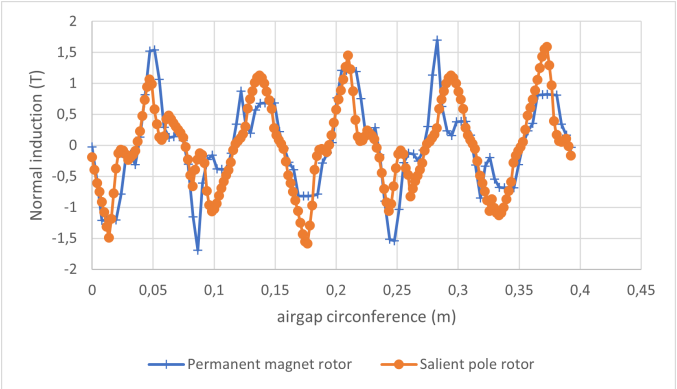

Fig. 4. Normal flux density comparison along an airgap lap

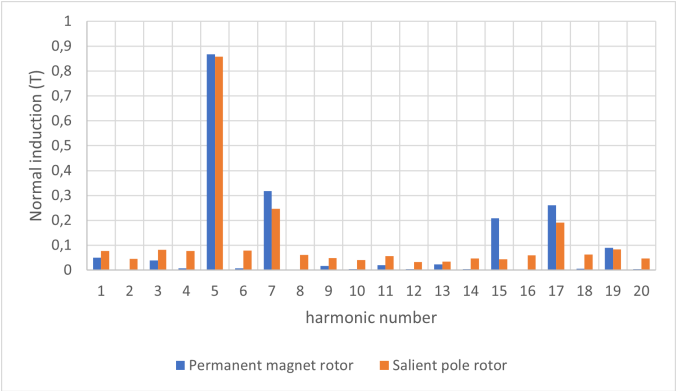

Fig. 5. Normal flux density spectrum comparison along an airgap lap

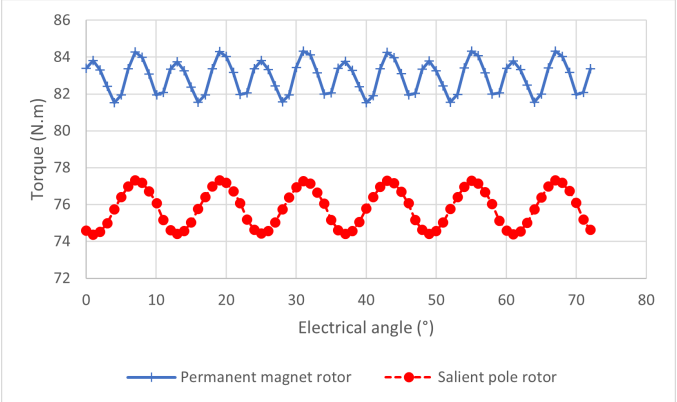

Fig. 6. Torque comparison at the rated operating conditions

3.2 Flux lines comparison

Fig. 7 and 8 present the mapping of flux lines for both machines. As it can be seen, the direction of the lines differs for the two rotors. They follow the pole in the radial way for the salient wound rotor whereas in the permanent magnet rotor they are oriented in an orthoradial way. This is due to the magnetization direction that enables to have a flux concentration machine. Therefore, only a part of the magnet flux crosses the airgap. The other part flows towards the shaft, and this part can be reduced using a special shape at the level of the magnet inner part as shown in Fig. 7.

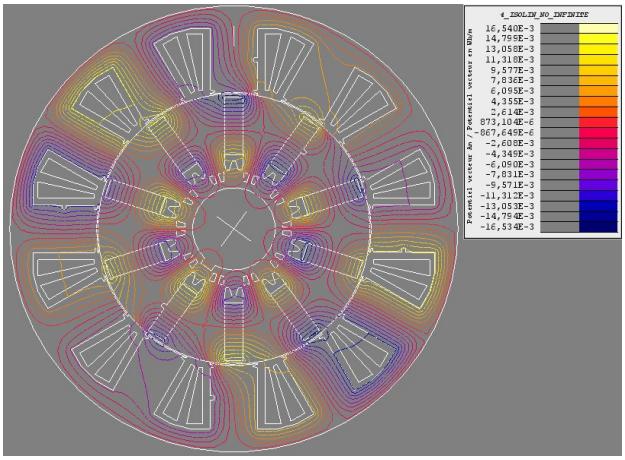

Fig. 7. Flux lines for the permanent magnet rotor machine

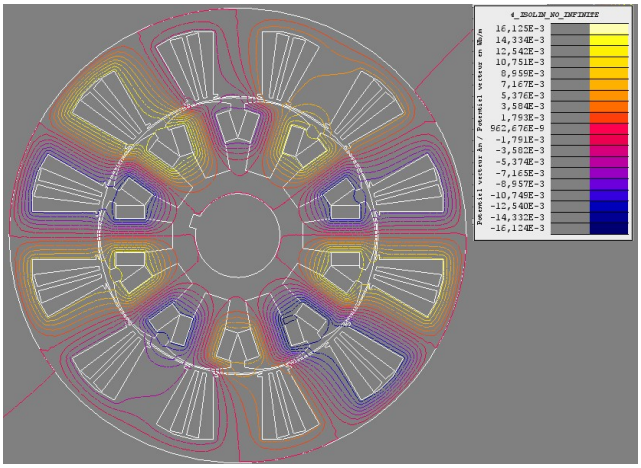

Fig. 8. Flux lines for the salient wound rotor machine

4 THERMAL STUDY

4.1 Power losses

Losses have been obtained with Flux2D software and are summed up in Table II. These values correspond to the rated point (4500 rpm and rated current as described in section 3).

TABLE II. LOSSES REPARTITION FOR BOTH MACHINES

Losses (W)	***Permanent magnet machine***	***Wound rotor machine***
Stator Joule	356	356
Rotor Joule	None	1827
Magnet	91	None
Stator iron	465	420
Rotor iron	76	48

Rotor Joule losses for the wound rotor seem to be quite important. This is due to the rotor direct current of 30 A which is injected in a thin aluminum tape. Thus, the rotor electric resistance is relatively high (around 2 Ω) which leads to high Joule losses. Comparatively, the stator current is higher (around 56 A RMS), but the tape is wider and shorter so with a small electric resistance.

4.2 Geometry for the thermal study using Motor-Cad software

The machines that have been designed using Flux2D software for the finite element study, have been rebuilt in the Motor-Cad software. Dimensions have been respected but some differences can be observed between Fig. 8 and 11 considering the head of rotor poles. The design has been adapted in Motor-Cad software to achieve the same performances (same torque) even if drawings are not identical. Indeed, Motor-Cad software can be used as a fast analytical electromagnetic predesign tool to get some data as the torque. However, because results are not obtained in the same way as with Flux2D, it doesn't lead exactly to the same values. Choice has been made to adapt the design to get the same torque because it is the main comparison indicator of the study. Furthermore, it has been verified that the impact of the slightly different design is not significant at all on thermal behaviour.

The other principal difference is the addition of a cooling part around the stator. This is a water jacket housing in a spiral. The characteristics of this cooling part are set to default in the software. An improvement of the cooling system could be made in further works.

4.3 Thermal results

From the losses in the different parts of the machines, a thermal study has been performed using Motor-Cad software. The ambient temperature is set to 20°C. The purpose is to evaluate the temperature range that could be attained at the most severe operating point. In a harsh environment with higher ambient temperature, machines would operate at reduced performances. In addition to losses repartition, the different materials are filled out (aluminum, steel and magnet) to get suitable thermal coefficients that are included in the software. Moreover, other characteristics, like interfaces behavior, are set to idle.

Table III presents thermal conductivity of the different materials used in both machines. These values are quite arbitrary because the exact composition of the machines that are being built is not known. However, because values from one steel alloy or aluminum alloy to another are very close, as a preliminary study, it has been considered that these coefficients are accurate enough to obtain representative results. Different values come from Motor-Cad database.

TABLE III. THERMAL COEFFICIENTS OF THE DIFFERENT MATERIALS

	Thermal conductivity (W/m/°C)
Aluminum winding	170
Stator lamination (M250-35A steel)	30
Rotor (stainless steel)	15
Magnet	8
Wire insulation (default)	0.2

Fig. 9, 10, 11 and 12 present temperatures at different critical points for both machines in axial and radial view.

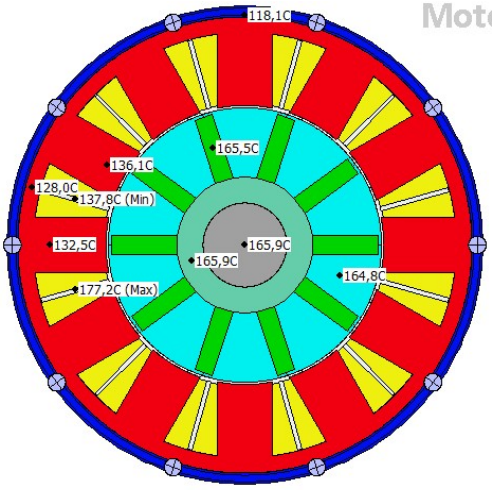

Fig. 9. Temperatures of the permanent magnet machine in radial view

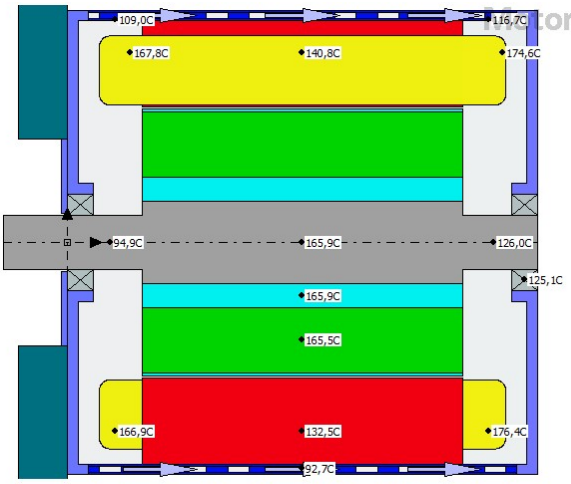

Fig. 10. Temperatures of the permanent magnet machine in axial view

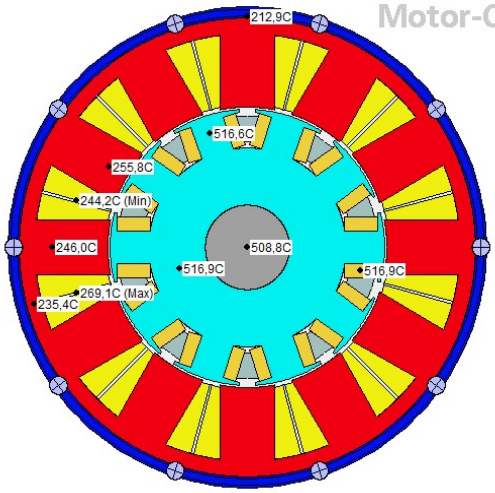

Fig. 11. Temperatures of the wound rotor machine in radial view

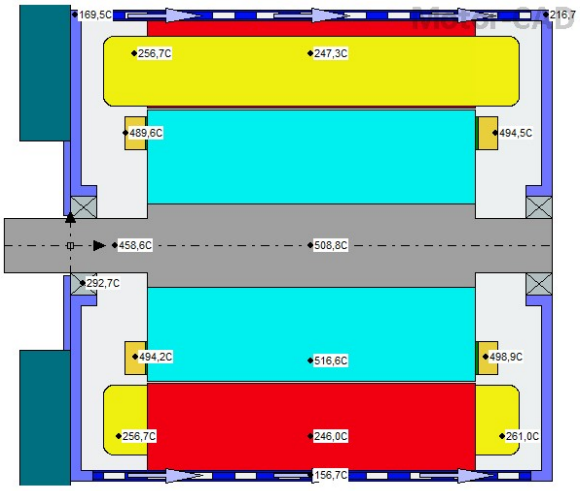

Fig. 12. Temperatures of the wound rotor machine in axial view

Presented results are given for steady state. This explains that temperatures can be rather high at specific critical points.

First, temperatures reached in the permanent magnet machine are quite usual (165.5°C) as it can be found in other studies [16]. This leads to be optimistic about the quality of the simulations, both for losses determination and the thermal study. Moreover, the maximal temperature in magnets is less than 170°C. This is clearly in the range of the selected magnets which are Samarium Cobalt-based. This kind of magnet can usually withstand up to 300°C [17].

Considering pure aluminum, the welding temperature is around 660°C. In the worst case, which is the wound rotor machine, the highest temperature reached is less than 520°C thanks to the cooling. It should be noticed that to simplify the simulation, the evolution of the electric resistivity of the aluminum with temperature has not been considered. It means that at 400 or 500°C the electric resistance of the tape would be higher, leading to even more losses, and higher temperatures. However, this machine has been designed to obtain the same performances with a wound rotor as with a permanent magnet rotor at least for short time.

Another point to be considered is the bearings temperature. Classical bearings are not suitable to withstand such temperatures (almost 300°C) [18]. So, in further works, a full study should be made to design bearings with innovative materials that could hold these temperatures. A specific rotor cooling system could also be implemented.

4.4 Study in transient

Steady state has been studied and it can be interesting to observe the evolution of some temperatures for a short period. This time the ambient temperature starts from 40°C. Fig. 13 and 14 present transient evolution of the temperature at different points on both machines for ten minutes.

First, concerning the permanent magnet rotor machine, only the stator winding is heating the most alongside the stator surface but in a reasonable range (≈ +40°C). This can be accounted for by stator Joule losses that are quite low thanks to a small electric resistance and because the cooling device is close to these windings. Also, the magnet and bearings stay at very low temperature which is a good result for the future testbench.

Concerning the wound rotor machine, the temperature rise of the stator winding is quicker and goes up to +70°C. Indeed, the losses of the rotor are higher and are the principal heating source of the machine. Moreover, the temperature in rotor windings rises also quickly. It reaches more than 300°C (starting at 40°C) after ten minutes. The interesting point is that even if the shaft heats up also significantly, bearings stay under 80°C until 5 minutes have passed, without considering the thermal inertia. This is reassuring concerning the experimental machine that is being built and it can be considered that tests could be executed for several minutes at rated operating conditions.

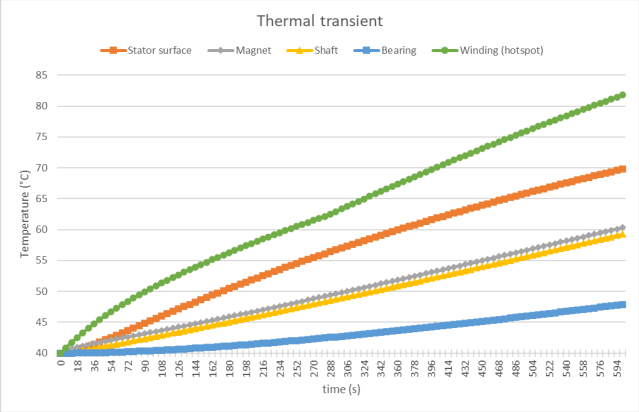

Fig. 13. Transient temperatures of characteristic points for the permanent magnet rotor machine

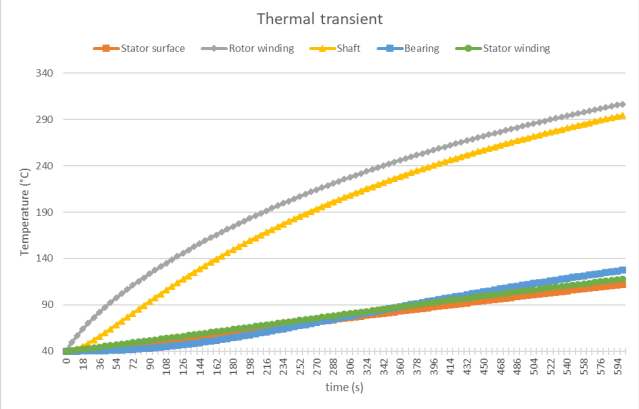

Fig. 14. Transient temperatures of characteristic points for the wound rotor machine

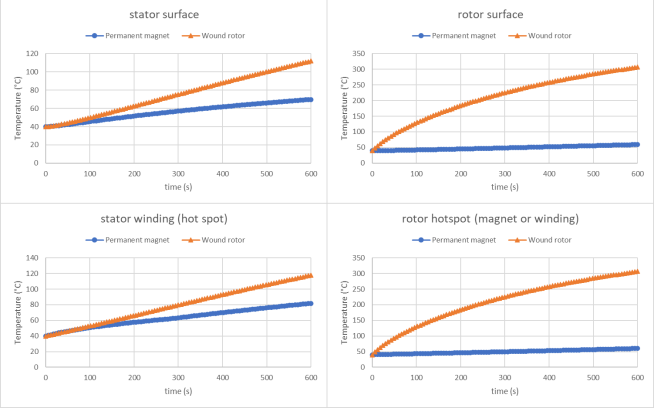

Fig. 15. Transient temperature comparison of characteristic points for both machines

Fig. 15 presents a comparison of transient temperature evolution for some characteristic points between both machines. Temperatures in wound rotor machine rise quicker than for the permanent magnet one. Stator rising temperature is almost linear while it starts to inflect on the rotor side. Even if results are not shown here, transient study showed that the steady state occurs after one hour and a half at rated operating conditions.

4.5 Thermal improvement in steady state

It has been shown previously that steady state temperatures for the wound rotor machine are quite high and would be even higher by considering the electric resistance increase. This could cause insulation deterioration or even critical failure in rotor windings.

To prevent any risk, a simple way to limit the heating is to decrease rotor direct current. In this case, airgap flux density will be lower than in the permanent magnet rotor machine. So, the stator current needs to be increased to compensate and to obtain the same torque. By coupling losses and thermal analysis with simple mathematical considerations, new configurations are obtained. Table IV sums up the results and compares values for the critical points which are stator and rotor windings. There is a quite noticeable impact on stator iron losses, but not on rotor iron losses.

As it can be observed, decreasing the rotor direct current by only 5 A leads to more than a 100°C reduction in windings rotor. An interesting fact is that even if stator current has been increased to get the same torque, stator temperatures are also lower. This means that for the wound rotor machine, heating is largely due to rotor losses. Moreover, the cooling water jacket is close to the stator so, it is easier to evacuate the heat in this area.

A very important result can be observed for the configuration 3, it is the optimum. Indeed, configuration 3 can be considered as the best because this is where stator temperature starts to inflect while rotor temperature is still decreasing. Moreover, configuration 4 demands a really high stator current. Configuration 3 presents the most balanced losses distribution and temperatures are much more convenient.

TABLE IV. COMPARISON OF DIFFERENT CONFIGURATIONS FOR THE WOUND ROTOR MACHINE

Configuration	***1***	***2***	***3***	***4***
Current rotor I_r	30 A	25 A	20 A	15 A
Current stator (peak) I_s	80 A	92 A	112 A	157 A
Rotor Joule losses	1800 W	1264 W	812 W	458 W
Stator Joule losses	356 W	471 W	700 W	1372 W
Stator iron losses	420 W	420 W	425 W	538 W
Rotor iron losses	48 W	48 W	48 W	48 W
Torque (average)	76 Nm	77 Nm	77 Nm	76 Nm
Rotor highest temperature (winding)	517°C	406°C	329°C	309°C
Stator highest temperature (winding)	269°C	237°C	223°C	263°C

4.6 Thermal results considering a harsh environment

As mentioned earlier, the purpose is to design a synchronous machine without magnet that could operate at

high temperature. Studies have been made at classical ambient temperature (20°C) in order to see the attained temperature range. With the improvement presented in the last subsection, it is interesting to evaluate what could happen in a harsh environment like in car or aircraft applications where ambient temperature is higher. As indicated in [19], the temperature range for the aircraft industry is very wide (from -55°C to 200°C). To stay relatively representative, the following study has been made with an ambient temperature of 150°C.

A simple way to extrapolate precedent results with a new ambient temperature is to reevaluate losses at 150°C. Concerning Joule losses, aluminum electrical resistivity is the only parameter to increase. In [20], the aluminum temperature coefficient is around 0.004 1/°C, this means that from 20°C to 150°C, resistivity increases by approximatively 50% and so do the Joule losses.

On the other way, [21] shows that iron losses decrease with temperature because both hysteresis and Eddy current loss coefficients are decreasing. This is also dependent to flux density, but the choice has been made to consider a 20% decrease for iron losses from 20°C to 150°C. Table V compares results obtained for the configuration 3 presented before for both ambient temperatures (20°C and 150°C).

As could be expected, the hotspots for both rotor and stator raise a higher temperature because global losses and ambient temperature are higher. It should be noted that when stator and rotor windings are at 300°C or more, the aluminum electrical resistivity is even higher and the same applies to the Joule losses. As explained before, a steady state operating condition at high temperature could lead to reducing the machine performances, but a transient operation (several minutes) could be achieved without any problem as shown in the transient study.

TABLE V. IMPACT OF AMBIENT TEMPERATURE FOR THE CONFIGURATION 3

Ambient temperature	***20°C***	***150°C***
Rotor Joule losses	700 W	1050 W
Stator Joule losses	812 W	1218 W
Stator iron losses	425 W	340 W
Rotor iron losses	48 W	38 W
Rotor highest temperature (winding)	329°C	539°C
Stator highest temperature (winding)	223°C	387°C

5 ROTOR WINDING REALIZATION

As previously explained, the winding is quite unusual because it is made of anodized aluminum tape. So, it is interesting to present technical solutions that have been chosen to make the windings, especially concerning the rotor.

First, rotor windings are coiled up around a plot corresponding to a rotor pole. Then, each plot will be screwed to the main piece of the rotor. Fig. 15 shows one plot with the anodized aluminum tape around. In the final version, each winding will be protected with fiberglass paper and filled up with a high temperature resin to ensure good rigidity and isolation. Because this kind of tape is relatively brittle and the rotor will turn up to 4500 rpm, a solution has been developed to ensure good stability and to connect the ten poles together. This is achieved with a connection disk attached to the rotor. One part of the tape goes through the disk and is screwed to the part of the tape from the direct next pole. Concerning the two parts of tape in contact on the disk, the anodized isolated surface has been removed. The disk is made in PEEK which is a polymer with good structural characteristics and a high welding point (343°C) [22]. Fig. 16 presents the connectivity principle on the disk. The same idea has been developed for stator connectivity.

Fig. 16. Example of winding around a pole rotor

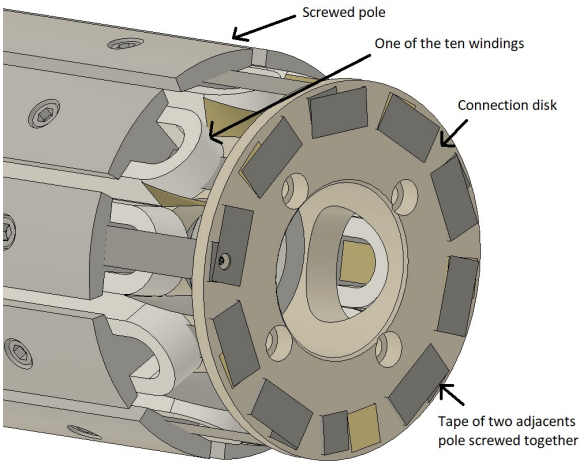

Fig. 17. Connection disk for the rotor winding

6 CONCLUSIONS AND PERSPECTIVES

This paper proposes a design of synchronous machines with the purpose to obtain the performances of PMSM with a salient pole wound rotor machine that can operate at higher temperature.

First, a sizing method has been presented and main dimensions have been given. Also, the way to find the ideal winding sequence has been presented.

Then, finite element simulations have been carried out with Flux2D software to compare the performances of the two machines with the same stator configuration. It appears that the obtained torque is quite similar with a small

advantage for the permanent magnet rotor machine. This has been explained previously.

Thanks to these simulations, Joule losses and iron losses have been determined and used in the Motor-Cad software to evaluate temperatures in steady state for an ambient temperature of 20°C. A transient study has also been proposed. It appears that the permanent magnet rotor machine ends with totally acceptable temperatures especially concerning magnets. However, temperatures reached in the wound rotor machine are relatively high and could deteriorate the machine especially the insulation in rotor windings. So, other configurations have been presented by decreasing rotor direct current and increasing stator current. Results show a better heat repartition and an optimum configuration while performances are not altered. A study has also been carried out for a higher ambient temperature with relevant results. Problems concerning some exterior parts such as classical bearings that cannot handle such temperature have been evocated. Moreover, the transient study has shown that machines could operate at rated conditions for several minutes without any risks.

From a technical point of view, the way to create winding with anodized aluminum tape has been shown.

Finally, design and simulated results have been conducted successfully with promising results to get a high temperature machine with great performances while avoiding magnets and classical winding that are not suitable with such temperatures.

Future works will consist of testing these machines which are currently being built in real conditions. Moreover, a study about the efficiency of both machines needs to be carried out and the environmental impact of these two technologies needs to be evaluated.

ACKNOWLEDGMENTS

This work has been achieved within the framework of CE2I project (Convertisseur d'Energie Intégré Intelligent). CE2I is co-financed by European Union with the financial support of European Regional Development Fund (ERDF), French State and the French Region of Hauts-de-France.

AUTHOR CONTRIBUTION STATEMENT

R. Cousseau and R. Romary conceptualized the study and developed the methodology. R. Cousseau performed design, simulations, analyses and wrote the manuscript. F. Balavoine helped for the thermal study analysis. R. Pusca and M. Irhoumah validated results and worked on the winding manufacture. All authors brang feedback and advises on the manuscript.

REFERENCES

[1] M. Lefik, K. Komeza, E. Napieralska Juszczak, D. Roger, P. Napieralski, N. Takorabet and H. Elmadah, "High temperature machines: topologies and premilinary design," De Gruyter, Open Phys. 2019, 17: pp. 657-669, doi: 10.1515/phys-2019-0068

[2] Z. Q. Zhu and D. Howe, "Electrical machines and drives for electric, hybrid, and fuel cell vehicles," Proceedings of the IEEE, 2007, vol. 95, no. 4, pp. 746–765, doi: 10.1109/JPROC.2006.892482

[3] M. N. Uddin, T. S. Radwan, and M. A. Rahman, "Performance of interior permanent magnet motor drive over wide speed range," in IEEE Transactions on Energy Conversion, vol. 17, no. 1, pp. 79-84, March 2002, doi: 10.1109/60.986441

[4] T. Huber, W. Peters and J. Böcker, "Monitoring critical temperatures in permanent magnet synchronous motors using low-order thermal models," IPEC-Hiroshima 2014 - ECCE Asia, Hiroshima, Japan, 2014, pp. 1508-1515, doi: 10.1109/IPEC.2014.6869785

[5] L. Marcin, K. Komeza, E. Napieralska-Juszczak, D. Roger, and P. Napieralski, "Comparison of the reluctance laminated and solid rotor synchronous machine operating at high temperatures," COMPEL - The international journal for computation and mathematics in electrical and electronic engineering, 2019, doi: 10.1108/COMPEL-10-2018-0405

[6] A. Vannini, A. Marfoli, L. Papini, P. Bolognesi and C. Gerada, "Materials for Electric Machines Suited for High-Temperature Applications: a Survey," 2021 IEEE Workshop on Electrical Machines Design, Control and Diagnosis (WEMDCD), Modena, Italia, 2021, pp. 101-106, doi: 10.1109/WEMDCD51469.2021.9425639

[7] A. Laidoudi, S. Duchesne, F. Morganti, and G. Velu, "High-power density induction machines with increased windings temperature," Open Phys., vol. 18, no. 1, pp. 642–651, 2020, doi: 10.1515/phys-2020-0131

[8] V. Iosif, D. Roger, S. Duchesne, D. Malec. "Assessment and improvements of inorganic insulation for high temperature low voltage motors," IEEE Transactions on Dielectrics and Electrical Insulation, 23(5), pp. 2534-2542, 2016, doi: 10.1109/TDEI.2016.7736810

[9] D. Roger, S. Duchesne, V. Iosif. "Magnetic characterization of the nickel layer protecting the copper wires in harsh applications," Archives of Electrical Engineering, 66, pp. 253-263, 2017, doi: 10.1515/aee-2017-0019

[10] D. Roger, H. Elmadah, and N. Takorabet, "Design of inorganic coils for high temperature electrical machines," Open physics, 2019, doi: 10.1515/phys-2019-0072

[11] S. Babicz, S. Ait-Amar, G. Velu, A. Cavallini, P. Mancinelli; "Behavior of anodized aluminum strip under sine and square wave voltage," IEEE Transactions on Dielectrics and Electrical Insulation, 24(1), pp. 39-46, 2017, doi: 10.1109/TDEI.2016.005834

[12] S. Babicz, S. Ait-Amar Djennad, and G. Velu, "Preliminary study of using anodized aluminum strip for electrical motor windings," IEEE Conference on Electrical Insulation and Dielectric Phenomena (CEIDP). IEEE, Des Moines, IA, USA, 2014, doi: 10.1109/CEIDP.2014.6995808

[13] S. Babicz, S. Ait-Amar, and G. Velu, "Dielectric characteristics of an anodized aluminum strip," IEEE Transactions on Dielectrics and Electrical Insulation 23.5, 2016, pp. 2970-2977, doi: 10.1109/TDEI.2016.7736860

[14] B. Cassoret, J. P. Lecointe and J. F. Brudny, "Influence of the Pole Number on the Magnetic Noise of Electrical AC Machines," Progress In Electromagnetics Research B. 2011, pp. 83-97, doi: 10.2528/PIERB1106200

[15] F. Libert and J. Soulard, "Investigation on pole-slot combinations for permanent-magnet machines with concentrated windings," International Conference on Electrical Machines, Cracow, Poland, January 2004, pp. 5–8.

[16] G. Guedia Guemo, P. Chantrenne and J. Jac, "Application of Classic and T Lumped Parameter Thermal Models for Permanent Magnet Synchronous Machines," International Electric Machines & Drives Conference, Chicago, IL USA, 2013, pp. 809-815, doi: 10.1109/IEMDC.2013.6556186

[17] J. F. Liu and M. H. Walmer, "Thermal stability and performance data for SmCo 2:17 high-temperature magnets on PPM focusing structures," IEEE Transactions on Electron Devices 52, 2005, pp. 899-902, doi: 10.1109/TED.2005.845868

[18] J.A. Henao-Sepulveda, M. Toledo-Quiñones and Y. Jia, "Contactless Monitoring of Ball Bearing Temperature," Instrumentation and Measurement Technology Conference, Ottawa, Canada, 17-19 May, 2005, pp. 1571-1573, doi: 10.1109/IMTC.2005.1604416

[19] K. E. Falahi, S. Hascoët, C. Buttay, P. Bevilacqua and L. V. Phung, "High temperature, Smart Power Module for aircraft actuators," HiTEN'13, Oxford, United Kingdom, 2013, hal-00874666

[20] D. C. Giancoli, "Physics principles with applications," 4th edition, 1995, Prentice Hall

[21] S. Xue, J. Feng, S. Guo, J. Peng, W. Q. Chu and Z. Q. Zhu, "A New Iron Loss Model for Temperature Dependencies of Hysteresis and Eddy Current Losses in Electrical Machines," in IEEE Transactions

on Magnetics, vol. 54, no. 1, pp. 1-10, 2018, Art no. 8100310, doi: 10.1109/TMAG.2017.2755593

[22] S. Xiaoyong, C. Liangcheng, M. Honglin, G. Peng, B. Zhanwei and L. Cheng, "Experimental Analysis of High Temperature PEEK Materials on 3D Printing Test," 9th International Conference on Measuring Technology and Mechatronics Automation (ICMTMA), Changsha China, 2017, pp. 13-16, doi: 10.1109/ICMTMA.2017.0012